NIH Public Access
Author Manuscript
Biomaterials. Author manuscript; available in PMC 2012 February 1.

Published in final edited form as:
Biomaterials. 2011 February ; 32(4): 1002–1009. doi:10.1016/j.biomaterials.2010.10.020.

Hydrogels with Time-Dependent Material Properties Enhance Cardiomyocyte Differentiation *In Vitro*

Jennifer L. Young and **Adam J. Engler***
Department of Bioengineering, University of California, San Diego; La Jolla, CA 92093

Abstract

Tissue-specific elastic modulus (*E*), or 'stiffness,' arises from developmental changes in the extracellular matrix (ECM) and suggests that progenitor cell differentiation may be optimal when physical conditions mimic tissue progression. For cardiomyocytes, maturing from mesoderm to adult myocardium results in a 9-fold stiffening originating in part from a change in collagen expression and localization. To mimic this temporal stiffness change *in vitro*, thiolated-hyaluronic acid hydrogels were crosslinked with poly(ethylene glycol) diacrylate, and their dynamics were modulated by changing crosslinker molecular weight. With the hydrogel appropriately tuned to stiffen as heart muscle does during development, pre-cardiac cells grown on collagen-coated HA hydrogels exhibit a 3-fold increase in mature cardiac-specific markers and form up to 60% more maturing muscle fibers than they do when grown on compliant but static polyacrylamide hydrogels over 2 weeks. Though ester hydrolysis does not substantially alter hydrogel stiffening over 2 weeks *in vitro*, model predictions indicate that ester hydrolysis will eventually degrade the material with additional time, implying that this hydrogel may be appropriate for *in vivo* applications where temporally changing material properties enhance cell maturation prior to its replacement with host tissue.

Keywords

Elastic Modulus; Hyaluronic Acid; Cardiomyocytes; Time-Dependent

1. Introduction

Cell behavior on compliant hydrogels often more closely approximates *in vivo* behavior compared to cells on rigid culture substrates, e.g. glass or plastic [1]. This occurs in part because cells can 'feel' that the hydrogel's elastic modulus (*E*), or 'stiffness' (measured in Pascal, Pa) more closely matches their native microenvironment as they contract against it. Mechanically-regulated responses are numerous but can include even the most fundamental processes, such as stem cell maturation [2–4], where muscle markers emerge in stem cells grown on hydrogels of muscle stiffness. Moreover, stiffness can affect tissue morphogenesis [5,6], e.g. tube formation [7], or migration of cells within explants [8]. Such behavior may also provide a mechanical explanation for the concept of 'tissue affinity,' where cells differentially sort within the body to form larger structures [9]. Yet over this time period in

*Corresponding author: Phone: (858) 246-0678, Fax: (858) 534-5722, aengler@ucsd.edu, Dept. of Bioengineering, University of California, San Diego, 251 Powell-Focht Bioengineering Hall, 9500 Gilman Drive, MC 0412, La Jolla, CA 92093 USA.

Publisher's Disclaimer: This is a PDF file of an unedited manuscript that has been accepted for publication. As a service to our customers we are providing this early version of the manuscript. The manuscript will undergo copyediting, typesetting, and review of the resulting proof before it is published in its final citable form. Please note that during the production process errors may be discovered which could affect the content, and all legal disclaimers that apply to the journal pertain.

NIH-PA Author Manuscript
NIH-PA Author Manuscript
NIH-PA Author Manuscript

NIH-PA Author Manuscript

NIH-PA Author Manuscript

NIH-PA Author Manuscript

which cells sort, they also secrete and assemble their extracellular matrix (ECM) [10], and together they gives rise to the stiffness associated with mature tissues [6,11].

Mature, contractile heart cells, i.e. cardiomyocytes, have traditionally be cultured on thick collagen gels to maintain rhythmic contraction [12,13], but more recently it was shown with synthetic gels [14] that stiffness is a critical regulator of contraction. This may be due in part to its modulation of cytoskeletal assembly in the form of myofibril striation and alignment, both of which can affect beating rate [15,16]. As with most other cell types [1], these behaviors in culture become most *in vivo*-like when cells are grown on a substrate which mimics the stiffness of their native environment. For example on a 10 kPa hydrogel, which mimics adult myocardial stiffness [17] and is similar to other muscle types [18–20], intra- and extra-cellular strains become matched and can prolong rhythmic beating in culture [16]. When too stiff or soft, cardiomyocytes overstrain themselves or do little work on the substrate, respectively, which in both cases result in few striated myofibrils and a loss of rhythmic contraction. In fact many diseases also stiffen the ECM, e.g. fibrotic stiffening of heart muscle post-heart attack [17], and induce hyper-strained myocytes that do not function properly. When coupled with stem cells for therapeutic use, failure to consider the altered material properties of disease can lead to undesired outcomes including the formation of calcified lesions [21], which emphasizes the importance of the mechanical properties of materials in regulating cell contraction.

Despite improved myocyte function on materials with biomimetic stiffness, the heart does not begin as a contractile 10 kPa material but instead originates from a much softer tissue layer call mesoderm < 500 Pa [22], which can require up to two weeks to develop in chicken [23,24]. In general though maturation from mesoderm to myocardium can require some finite amount of time and suggests that rigid or even soft materials with static properties, e.g. thick collagen [12,13] or synthetic gels [14–16], may not provide the most appropriate physical environment in which to study stem or progenitor cells *in vitro*. While the kinetics of stiffening are uncertain, development of immature cells into cardiomyocytes is likely due in part to this time-dependent mechanical change from softer mesoderm into stiffer heart tissue [25]. This then supports the appropriate level of tension required to assemble an adequate amount of myofibrils, i.e. the contractile unit of muscle [13]. However, no biologically-appropriate material has been demonstrated to exhibit time-dependent stiffening in which to test this hypothesis, especially one that is tuned to mimic the mechanics of developing myocardium. Since immature cells require muscle-like stiffness in which to develop into muscle [3] as opposed to the rigid, fibrotic tissues in which they are often used therapeutically [17,21], understanding the effect of time-dependent stiffening on cell maturation may be a critical design parameter for future material-based therapies that involve the addition of co-injected cells.

2. Materials and Methods

2.1 Materials

Hyaluronic Acid (HA) was obtained from Calbiotech (CA) and thiolated using a cleavable, carbohydrate selective, sulfhydryl-reactive crosslinker, PDPH (3-[2-Pyridyldithio]propionyl hydrazide) (Thermo Scientific-Pierce), MES Buffer (Thermo Scientific-Pierce), DMSO (Sigma), EDC (1-ehtyl-3-[3-dimentylaminopropyl] carbodiimide hydrochloride) (Sigma), and DTT (dithiothreitol, Sigma). Alternatively, thiolated HA of similar functionality was also obtained from Glycosan Biosystems (UT). Poly(ethylene glycol) diacrylate (PEGDA) of different molecular weight was used as a crosslinker (M_w ~ 3400 Da from Glycosan Biosystems, UT and M_w ~ 258, 700 and 2000 Da from Sigma). For protein attachment on gels, EDC, NHS (N-Succinylamide) (Sigma) and type I rat tail collagen (BD Biosciences) in HEPES buffer (Sigma) was used. Polyacrylamide (PA) hydrogels were prepared from cross-

NIH-PA Author Manuscript

NIH-PA Author Manuscript

NIH-PA Author Manuscript

linker *n,n′*-methylene-bis-acrylamide and acrylamide monomers (Fisher Scientific), and the same protein was covalently attached using a photoactivating cross-linker, sulfo-SANPAH (Pierce).

To fluorescently label collagen or cells on the surface of the hydrogel for imaging purposes, primary monoclonal mouse type I collagen antibody (C2456, Sigma), alpha-actinin (A7811, Sigma), rhodamine-phallodin, Hoescht (33342, Sigma) and Alexa Flour 488 or 568 conjugated goat anti-mouse secondary antibody (Invitrogen) were used. Samples were mounted using Fluoromount-G (SouthernBiotech). For ELISA, secondary goat anti-mouse HRP-conjugated antibody (62-6520, Zymed) and 3,3′,5,5′-Tetramethylbenzidine (TMB, Sigma) were used.

To examine myocardial stiffness and subsequent use in cell studies, chicken embryos were obtained from McIntyre Poultry Farm (Lakeside, CA). For histological analysis, hearts were embedded in optimal cutting temperature (OCT) solution (TissueTek) and stained using phosphomolybdic acid (Electron Microscopy Sciences-EMS), sirius red in 0.1% saturated picric acid (EMS), and mounted with Cytoseal (Richard Allen Scientific). For cardiomyocyte isolation, tissue was digested using 0.05% trypsin-EDTA (Invitrogen) and purified using a 70 μm cell strainer (BD Falcon). Cells were stored in normal heart medium (89% MEM alpha: L-glutamine (+), ribo-/deoxyribo-nucelosides (−), Invitrogen; 10% fetal bovine serum, Hyclone; and 1% penicilin:streptomycin, Invitrogen).

For reverse transcription PCR (RT-PCR), 10 mM dNTP (Roche), 100 mM DTT (Invitrogen), 5X First Strand Buffer (Invitrogen), 50 mM Random Hexamers (Qiagen), 200 U/μL Reverse Transcriptase (Invitrogen), DEPC water (OmniPur, EMD) were used. For quantitative PCR (qPCR), SYBR Green (Applied Biosystems) and primers obtained from Integrated DNA Technologies (IDT) (Table S1) were used.

2.2 Hyaluronic Acid Thiolation

Fermentation-derived HA (sodium salt) of intermediate molecular weight, e.g. 769 kD, was digested in order to obtain low molecular weight HA of M_w ~ 200 kD as previously described [26]. Briefly, 1 mg/mL HA was dissolved in 37°C water of pH 0.5 (adjusted by the addition of 10 M HCl) and mixed at 130 rpm for 6 hrs. pH was then adjusted to 7.0 with 1 M NaOH, dialyzed against water for 4 days (12 kD molecular weight cutoff), and centrifuged before the supernatant was lyophilizated. HA was dissolved in MES Buffer at 5–10 mg/mL. 25 μL of 20 mM PDPH in DMSO was added per 1 mL of HA solution. The reaction was carried out at room temperature for 30–60 minutes. 12.5 μL of 0.5 M EDC in MES buffer was added per 1 mL of HA solution. The solution was mixed and incubated at room temperature for 2 hours to overnight with mixing. The solution was centrifuged in order to remove any precipitate that formed during the reaction. Any non-reacted PDPH molecule was removed by dialysis or gel filtration. In order to reduce the disulfide bond, 0.5 mL of 23 mg/mL DTT in MES buffer was added per 1 mL of PDPH-modified HA and incubated for 30 min at room temp. The solution was dialyzed or gel filtered in order to remove any excess DTT. Samples were lyophilized, dissolved in D_2O at 1 mg/mL and analyzed via ^1H nuclear magnetic resonance (NMR) spectroscopy (JEOL ECA 500) to assess thiol substitution.

2.3 Gel Synthesis, Protein Attachment, and Detection

To prepare HA hydrogels of the appropriate stiffness to mimic heart stiffening, 4.53% (w/v) PEGDA with M_w ~ 3400 Da (polydispersity index or PDI ~ 3) in DG PBS and 1.25% thiolated HA in DG PBS were separately mixed at 37°C with gentle shaking for up to 30 minutes. For swelling experiments, PEGDA with M_w ~ 258 Da, 700 Da, and/or 2000 Da

NIH-PA Author Manuscript

NIH-PA Author Manuscript

NIH-PA Author Manuscript

(PDI ~ 1) were also used in a similar fashion. To initiate polymerization, solutions were combined at a volume ratio of 1 PEGDA solution: 4 HA solution to yield a 1% HA/0.9% PEGDA hydrogel, and 50 μL of the solution was placed between adhesive, aminosilanated and non-adhesive hydroxylated glass coverslips[27] and allowed to polymerize in a humidified 37°C incubator for 1 hr. Hydrogels bound to the aminosilanated coverslip were rinsed and stored in DG PBS in a humidified 37°C incubator until use. To attach protein to the surface, 20 mM EDC, 50 mM NHS and 150 μg/mL type I rat tail collagen were mixed in HEPES buffer and incubated with the hydrogels overnight. Polyacrylamide gels were prepared as described previously [27]. Briefly, gel cross-linker n,n′-methylene-bis-acrylamide and acrylamide monomer concentrations were varied in distilled water and polymerized between adhesive, aminosilanated and non-adhesive hydroxylated glass coverslips using 1/200 volume of 10% ammonium persulfate and 1/2000 volume of *n*,*n*,*n*′,*n*′-tetramethylethylenediamine. To attach protein to the PA hydrogel surface, 0.5 mg/ml sulfo-SANPAH (Pierce) in 50 mM HEPES pH 8.5.

Enzyme-linked immunosorbent assay (ELISA) was used to compare amount of rat tail type I collagen binding to HA and PA hydrogels when using optimal coating densities of 1 $\mu g/cm^2$ as previously described [27]. Primary monoclonal mouse type I collagen antibody was incubated at 1:500 in 2% ovalbumin with cells on hydrogels for 1 hr at 37°C. After rinsing, 1 mL of secondary goat anti-mouse HRP-conjugated antibody at 1:1000 and 1:5000 in 2% ovalbumin was added to the gel surface and incubated for 1hr at 4°C. After rinsing, 0.5 mL of TMB ELISA substrate was added and incubated at room temperature for 30 min. The reaction was stopped using 1 M HCl and analyzed on a plate reader at 450 nm. Binding was confirmed and assessed by immunofluorescence using a BD Carv II confocal microscope (BD Biosciences; San Jose, CA) mounted on a Nikon Eclipse TE2000-U microscope with Metamorph 7.6 software. Image brightness was uniformly enhanced 2-fold to better illustrate the location of labeled protein.

2.4 Material Stiffness and Surface Topography

Force-mode atomic force microscopy (AFM) was performed on the developing myocardium and HA and PA hydrogels to examine mechanical properties. For the tissue samples, specimens were isolated from chicken embryos, bisected, and mounted on glass slides with epoxy to expose the apical surface. HA and PA hydrogel bound to aminosilanated coverslips were directly mounted on the AFM stage (3D-Bio; Asylum Research). Samples were indented to a depth of 100 nm with a pyramid-tipped cantilever having a spring constant (20 pN/nm nominal) as determined from thermal calibration. At least 50 measurements were made randomly across the surface of each sample. Force-indentation plots were fit with a Hertz model to determine the Young's modulus [28]. To assess disulfide crosslinking, HA gels were treated with 0 mM, 1 mM and 1M DTT in order to examine disulfide bond formation during gelation. Data for the elastic modulus of HA gels and the myocardium were fit with exponential decay curves to assess differences between the systems. For HA and PA hydrogels, AFM was also performed in tapping mode to image surface topography.

2.5 Material Stability and Degradation

Degradation of HA hydrogels was determined via equilibrium mass swelling ratio (Q_m), thickness measurements, and elastic modulus effects. For Q_m, thickness measurements, and elastic modulus determination, degradation was carried out at 37°C in pH 7.4 and pH 9 PBS (enhanced degradative environment). For determination of Q_m, as defined by the ratio of swollen polymer to dry polymer, the weight of each sample was examined over time. At 24 hpp, multiple samples were weighed and then lyophilized in order to determine an average equilibrium swelling ratio. Swollen HA gels were weighed over time and Q_m values were calculated. We assume HA gels remain a constant material mass over the time points

NIH-PA Author Manuscript

NIH-PA Author Manuscript

NIH-PA Author Manuscript

examined (up to 2 weeks), as these times are less than that of significant degradation. Thickness measurements were examined over time after coating HA gels with collagen and fluorescently tagging and using confocal microscopy to measure distance from top of gel to top of coverslip. Stiffness measurements were collected as previously described for force-mode AFM but in the presence or absence of basic pH. Hydrogel modulus was examined as previously described for force-mode AFM.

2.6 Hydrolysis Modeling

One characteristic of PEGDA addition reactions is the formation of hydrolytically degradable esters, which may balance the stiffening effect of additional crosslinks. Metters and coworkers [29] previously reported an application of a Flory-Rehner hydrolytic degradation model, [30] which was used here to illustrate the kinetics of crosslinking versus ester degradation through a description of the change in hydrogel swelling. While Metters and coworkers describe a triblock system consisting of poly(lactic acid) (PLA) and PEG, i.e. PLA-PEG-PLA, where hydrolyzable ester bonds are found within PLA block, we can apply this system to the reaction of PEGDA with HA since it creates two degradable esters existing on opposite ends of the PEGDA crosslinker. Briefly, first order hydrolysis kinetics are assumed for ester bond degradation, having a pseudo first-order rate constant for ester bond hydrolysis, k'. The fraction of hydrolyzed thioether-ester groups, which form between the HA backbone and PEGDA crosslinker (P), is related to

$$P=1-e^{-k't} \tag{1}$$

The crosslinking density (ρ_c) as a function of time can then be related to (1) using knowledge of the triblock crosslink structure as follows

$$\rho_c \sim (1-P)^2 \sim e^{-2jk't} \tag{2}$$

Using a simplified form of the Flory-Reher equation, which relates volumetric swelling ratio (Q) to crosslinking density, Q can be related to time by

$$Q \sim \rho_c^{-0.6} \sim e^{1.2k't} \tag{3}$$

and plotted with experimentally-determined Q_m for the thiolated HA hydrogels between 0 and 216 hpp as shown in SFig. 3C. It is important to note that this model assumes immediate and complete crosslinking in equations (2) and (3), which describes crosslinking density only as it exponentially decays from hydrolysis. Since opposing behavior is observed initially for HA hydrogels, either additional crosslinking with time may reduce and delay hydrogel swelling or degradation kinetics are sufficiently slow as to be decoupled from additional crosslinking. Regardless, any hydrolysis-induced material erosion is not experimentally observable until after stiffening has occurred (Fig. 2C).

2.7 Cell and Tissue Isolation and Cell Culture

Animals received humane care in compliance with University of California, San Diego's Institutional Animal Care and Use Committee (protocol # S09200). Chicken embryonic hearts and heart cells were obtained by isolation at 72, 120, 168, 240 and 288 hpf. Age was confirmed using Hamburger-Hamilton stages [23]. Hearts were obtained by dissection and

NIH-PA Author Manuscript

NIH-PA Author Manuscript

NIH-PA Author Manuscript

either mounted for AFM or embedded in optimal cutting temperature (OCT) solution for histological analysis using a Picrosirius red stain. Briefly, after sectioning samples and mounting on glass slides, tissue was rehydrated, treated with 0.2% phosphomolybdic acid, stained with sirius red in 0.1% saturated picric acid, then 0.01M HCl, dehydrated, cleared and mounted with Cytoseal. For cardiomyocyte isolation, isolated hearts were minced using sterile razor blades and collected with 10 mL of 0.05% trypsin-EDTA (Invitrogen) and incubated in a sterile humidified 37°C incubator (5% CO_2) for 15 min. In order to remove red blood cells, the tube was inverted and tissue was allowed to settle prior to a change of solution to 10 mL of fresh trypsin. After incubation for 15 min, the sample was centrifuged and the pellet was carefully triturated with normal heart medium (89% MEM alpha: L-glutamine (+), ribo-/deoxyribo-nucelosides (−), Invitrogen; 10% fetal bovine serum, Hyclone; and 1% penicilin:streptomycin, Invitrogen). The cell solution was passed through a 70 μm cell strainer (BD Falcon) and pre-plated on a sterile tissue culture dish for 1 hr in a cell incubator in order to remove fibroblasts from the solution. The unattached cells were collected, counted, and plated at a density of 5×10^6 cells/cm^2. Cells used for qPCR and immunofluorescence were incubated according to the time course in Fig. 3. Media changes were performed every 2 days. All cell culture and tissue experiments were performed at least in triplicate.

2.8 Cell Maturation Assays

In order to examine cardiac ECM expression in the myocardium, chicken embryonic hearts were isolated and mRNA was extracted as follows. Cells on hydrogels were washed with PBS, lysed with trizol for 5 min at room temperature and the solution transferred to RNAase/DNAase-free eppendorf tubes. Chloroform was added and samples were vigorously shaken at room temp for 2 min. Samples were centrifuged in order to separate phases and the aqueous phase was transferred to new tubes. RNA was precipitated by the addition of isopropanol, vortexing and allowing samples to sit at room temperature for 10 min. The samples were then centrifuged, the supernatant was removed and a gel-like RNA pellet was washed with 75% ethanol and vortexed. The samples were spun a final time and the supernatant was removed. The RNA sample was allowed to air dry for 5 min. Samples were resuspended in DEPC water (OmniPur, EMD) and absorbance was examined for RNA concentration at 260 nm OD. In order to convert mRNA into cDNA for future analysis, reverse transcription polymerase chain reaction (RT-PCR) of 37°C for 60 min, followed by 99°C for 5 min, followed by 5°C for 5 min was performed. Samples consisting of 2 μg of mRNA were mixed with 20 μL of mastermix consisting of 1 μL 10 mM dNTP (Roche), 2 μL 100 mM DTT (Invitrogen), 4 μL 5X First Strand Buffer (Invitrogen), 1 μL 50 mM Random Hexamers (Qiagen), 1 μL 200 U/μL Reverse Transcriptase (Invitrogen) and 11 μL DEPC H_2O. qPCR was then performed using an Applied Biosystems 7900HT Fast Real-Time PCR machine for quantifying matrix protein expression of collagen (COL) 1A2, laminin (LN) 2 and fibronectin (FN) 1 (see Supplemental Table 1 for list of primers).

In order to examine cell maturation from the time course previously described, samples were either used to quantify cardiac gene expression or were stained with antibodies specific to cardiac proteins. Cardiac gene expression was determined via qPCR (as previously described) for Troponin T and MESP2 (see Supplemental Table 1 for list of primers). Immunofluorescence was performed as follows: cells were fixed with 3.7% formaldehyde in PBS for 15 min, rinsed and permeabilized using Triton X-100 for 10 min. Cells were rinsed and incubated with primary mouse antibody for alpha-actinin (A7811, Sigma) at 1:500 in 2% ovalbumin for 30–60 min in a 37°C cell incubator. Samples were rinsed and 1:1000 rhodamine-phallodin (R415, Invitrogen), 1:1000 Alexa Flour 488 conjugated goat anti-mouse secondary antibody (Invitrogen) and 1:5000 Hoescht (33342, Sigma) in 2% ovalbumin were added for 30 min at 37°C. Samples were rinsed and mounted with

NIH-PA Author Manuscript

NIH-PA Author Manuscript

NIH-PA Author Manuscript

Fluoromount-G (SouthernBiotech) and sealed with nail polish. Images were captured using a Nikon Eclipse TE2000-U fluorescent microscope with Metamorph 7.6 software. Images were analyzed using Image J to determine striation length by drawing a calibrated line through a fibril and dividing by the number of striations, and myofibril alignment by examining ellipse fits of fibrils and calculating the deviation of fibrils from long cell axis using an orientation correlation function (OCF): $OCF = 0.5 (\cos (2\theta) + 1)$, where θ is the difference between the angle of the fibril and cell axis.

2.9 Statistical Analyses

All statistical analyses were performed using student t-tests. Differences among groups were assessed to identify statistical differences between treatments when p is at least less than 0.05. Data where $0.05 < p < 0.1$ is indicated though not statistically different. All data is presented as mean ± standard error of the mean.

3. Results and Discussion

3.1 Characterization of Developing Myocardium

In order to test the hypothesis that time-dependent material properties can improve cell maturation, mechanochemical parameters of the developing heart were first characterized using a chicken embryo model, which displays all the hallmarks of human heart development [24] in distinct stages [23]. *Ex vivo* samples of the developing heart were isolated between 36 and 408 hours post-fertilization (hpf) of the embryo, mounted on a glass slide and an atomic force microscope (AFM) was used to indent the inner tissue surface and assess stiffness. Fig. 1A shows the developing embryonic chicken heart undergoes a 9-fold increase in elastic modulus, i.e. $E \sim 0.9 \pm 0.2$ kPa at 36 hpf to $E \sim 8.2 \pm 1.3$ kPa at 408 hpf, and an exponential curve fit of these data indicate a time constant, τ, of 57.6 hpf. One tissue component that changes significantly over this time course and may likely responsible for heart stiffening is the extracellular matrix (ECM), a protein scaffold to which cells attach and transduce signals; since cells attach to ECM rather than polymers, knowing what the most abundant ECM protein is may aid in attaching cells to the material. Quantitative polymerase chain reaction (qPCR) was used to assess compositional changes of heart ECM proteins, e.g. collagen, laminin, and fibronectin, over this developmental time course (Fig. 1B). Collagen expression increased through 264 hpf and changed from being peripherally-localized to be uniformly distributed (Fig. 1B inset). Though peripherally-localized collagen is likely mechanically important during heart formation [25], uniform collagen expression throughout the heart may enable a consistent set of material properties for heart maturation. On the other hand, both fibronectin and laminin expression decreased by almost an order of magnitude from 72 to 408 hpf and are not as likely to contribute to tissue stiffening as much as collagen may.

3.2 Mimicking and Monitoring Time-Dependent Stiffness in Hyaluronic Acid Hydrogels

We have used a modified hyaluronic acid (HA) hydrogel to recapitulate this dynamic environment *in vitro*. HA is a natural, non-immunogenic [31] ECM component that can be easily modified to display various chemistries [26,32,33]. HA was thiolated using the carbohydrate selective, sulfhydryl-reactive crosslinker (3-[2-Pyridyldithio]propionyl hydrazide) and upon reduction, a free thiol was added to the end of the carboxyl group (see Fig. S1A1). Substitution efficiency was confirmed by ^{1}H nuclear magnetic resonance (NMR) spectroscopy, comparing methylene peaks 1 and 2 and the *N*-acetyl methyl peak 3 in Fig. 2A to determine a ~40% average thiolation. A poly(ethylene glycol) diacrylate (PEGDA) crosslinker was added to initiate a Michael-type addition reaction [34] (Fig. S1A2). Addition reaction dynamics can be controlled by PEGDA molecular weight: hydrogels composed of higher molecular weight PEGDA reduced their mass swelling ratio,

NIH-PA Author Manuscript

NIH-PA Author Manuscript

NIH-PA Author Manuscript

i.e. the ratio of swollen to dried polymer weight (Q_m, Fig. 2B), and stiffened (Fig. 2C) faster than lower molecular weight PEGDA hydrogels. This could imply that a higher molecular weight PEGDA bound at one end may diffuse through greater space and thus is more likely to find an unbound thiol site faster to form a crosslink.

To obtain a hydrogel that stiffened similarly to heart, 0.9% PEGDA of M_w ~ 3400 Da and 1% thiolated HA were polymerized into hydrogel, characterized via AFM over 456 hours post-polymerization (hpp), and found to stiffen from 1.9 ± 0.1 to 8.2 ± 1.1 kPa (Fig. 2C) with a time constant of 69.6 hpp. Due to the presence of free thiol groups however, it is possible that some of the time-dependent stiffness could be due to the formation of disulfide bonds between adjacent thiolated HA chains and not the Michael-type addition reaction. Therefore HA hydrogel stiffness was measured in the presence of 1 mM and 1 M dithiothreitol (DTT), a reducing agent of disulfide bonds. The addition of 1 mM DTT, a concentration which normally reduces protein disulfides, had a negligible effect on HA hydrogel stiffness over time compared to untreated hydrogels. 1 M DTT appears to interfere with stiffening (Fig. 3), but the high concentration may affect many other hydrogel properties. Thus it would appear that a time-dependent Michael-type addition reaction is the likely candidate for the majority of stiffening observed here.

Hydrogel degradation via ester hydrolysis, which would actually soften the hydrogel, could compete with time-dependent crosslinking that stiffens the material. Degradation over a cell-relevant time course was monitored by placing hydrogels in either neutral (pH 7.4) or basic (pH 9) degassed (DG) PBS, the latter of which is an enhanced degradative environment for esters. Hydrogel stiffness at pH 9 was significantly lower than neutral pH, but only after more than 300 hpp (Fig. 4A)–the point at which stiffening plateaus (see Fig. 2C)–indicating that even in hydrolyzing environments, significant time must elapse before degradation out competes crosslinking to soften the material. However, degradation might cause material erosion rather than affect micro-scale stiffness, so hydrogel thickness, surface topography, and swelling were examined in neutral and basic conditions. The z-position of fluorescently-labeled collagen that was covalently bound to the hydrogel surface was monitored using confocal microscopy (see Fig. S2B inset), and over 288 hpp, the z-position of this layer on the HA hydrogel surface decreased more than ~45% in basic conditions indicating hydrogel thinning. Changes in neutral pH were more modest indicating less thinning (Fig. 4B). Substrate topography, which can significantly affect cell responses [35], may be affected by hydrolysis-induced material erosion. Yet surface roughness, i.e. the root mean squared height change along the hydrogel surface (Fig. 5A), did not change for HA hydrogels between 24 and 192 hpp (Fig. 5C). However material erosion, if any, may be best reflected by changes in swelling [30]. Measurements of the equilibrium mass swelling ratio (Q_m) showed that the HA samples regardless of pH decreased Q_m through 144 hpp and then maintained low Q_m up to 288 hpp. Such behavior is unlike the exponential increase predicted by the Flory-Rehner model for similar hydrogel systems using modest hydrolysis rate estimates where bond hydrolysis increases hydrogel water content [29,36] (Fig. 4C). The difference may be due to that model's assumption of immediate and complete crosslinking; evidence here would suggest that complete crosslinking is not achieved until at least 216 hpp resulting in decreased Q_m with the presence of less water in the hydrogel. Thus any hydrolysis-induced erosion must at least be equally balanced with additional crosslinking through 288 hpp, but after which time hydrolysis may dominate.

In contrast to time-dependent hydrogels, polyacrylamide (PA) hydrogel crosslinking is provided by persulfate-generated free radical polymerization (Fig. S1B). This creates hydrogels with stiffness which remains constant over time (Fig. S2A; grey circles), making it a suitable control for HA hydrogels. However, both hydrogels require the attachment of ECM protein to facilitate cell adhesion. Type I collagen was covalently linked to the

NIH-PA Author Manuscript

NIH-PA Author Manuscript

NIH-PA Author Manuscript

hydrogel surfaces using NHS chemistry, and to ensure similar attachment on both hydrogels, an enzyme-linked immunosorbent assay (ELISA) was performed. Despite the different surface chemistry, PA hydrogels contained only 23.1 ± 1.9 % more collagen than HA hydrogels (Fig. S2B), and confocal cross sectional images show that fluorescently-labeled collagen is evenly distributed along the tops of both hydrogels (Fig. S2B inset), suggesting that the surfaces may appear to be similar to cells.

3.3 Improved Cardiac Progenitor Cell Marker Expression on Hydrogels with Time-Dependent Stiffness

To examine to what extent material stiffening regulates cardiomyocyte development, embryonic cells were isolated from myocardial or precursors tissues at 72, 120, 168, 240, and 288 hpf and cultured *in vitro* on both hydrogel systems until reaching a total age of 312 hpf. Cells isolated at each time point were plated on hydrogels of appropriate elastic modulus for that specific time point, i.e. cells plated at 72 and 288 hpf were cultured on 1 and 8 kPa hydrogels, respectively, to match previously determined tissue elastic modulus measurements with the only difference being that PA hydrogels did not stiffen while HA hydrogels continued to stiffen over time. Over this time course, expression of the immature marker NKX-2.5 and the mature cardiac specific marker Troponin T were first monitored in the intact heart and found to decrease and increase, respectively (Fig. S3). After 312 hpf, Troponin T expression, normalized to final tissue expression, was 3-fold higher on HA than PA hydrogels in cells isolated before 150 hpf (Fig. 6A bottom). Expression of NKX-2.5, normalized to already low expression in the animal at late time points, was less than 1 (Fig. 6A top), indicating that all young, pre-cardiac cells had reduced expression of immature markers but only cells grown on HA hydrogels expressed mature cardiac markers. A better assessment of cardiac muscle formation, however, is the assembly of contractile units, i.e. myofibrils, which show a striped pattern of alternating actin and myosin. These fibrils can be described by three major stages to indicate muscle maturity: premyofibrils, maturing myofibrils, and mature myofibrils where the alternating pattern is less than 1 μm, 1 – 1.8 μm, and 1.8 – 2.2 μm [13], respectively, as is illustrated in Fig. 6B with staining for actin and cardiac specific α-actinin. Though all cells stained positively for cardiac specific α-actinin, quantifying myofibril striation distance indicated that greater than 75% of pre-cardiac cells plated on HA hydrogels contained maturing or mature myofibrils for cells isolated before 150 hpf (Fig. 6C). Conversely, pre-cardiac cells on PA hydrogels mostly contained premyofibrils (40 – 85 %) at these early time point, resulting in up to a 60% difference. Myofibril alignment with each other and the long axis of the cell is also an indication of muscle maturity [13] (Fig. 7A) and was quantified via an orientation correlation function (OCF) [37]; when OCF is 1, fiber alignment is in the direction of the long axis of the cell and when close to 0, orientation is misaligned, i.e. perpendicular to the cell axis. The OCF of cells grown *in vivo* for the longest time examined, i.e. 244 hpf, showed that cells had the highest alignment, consistent with the most mature cells coming directly from the animal. Yet again for cells isolated before 168 hpf, HA hydrogels produced cells with better aligned myofibrils compared to PA hydrogels as OCF was consistently higher (Fig. 7B).

4. Conclusions

In vitro studies presented here demonstrate the importance of dynamic material cues in guiding cell maturation while modeling implies that this hydrogel may be appropriate for *in vivo* applications due to its eventual but not immediate hydrolysis. Moreover, this study illustrates the importance not just of material properties as design criterion for therapies but of how these properties change during development, an especially critical point when a therapy intends to produce mature cells from immature precursor cells. Despite tuning HA

NIH-PA Author Manuscript

NIH-PA Author Manuscript

NIH-PA Author Manuscript

hydrogel stiffening to mimic the mechanics of heart development here, developmental changes that lead to tissue stiffening occur ubiquitously, and this HA-based system can likely be tuned to match stiffening that occurs in many other biological contexts.

Supplementary Material

Refer to Web version on PubMed Central for supplementary material.

Acknowledgments

The authors would like to thank Dr. Donald Elbert (Washington University in Saint Louis) for advice with degradation modeling, Dr. Jean Sanger (Upstate Medical University) for assistance with cardiomyocyte isolation, Dr. Jason Li (Asylum Research) and Mr. Somyot Chirasatitsin for technical assistance with atomic force microscopy, Dr. Anthony Mrse for assistance with NMR spectroscopy. This work was supported by grants from the American Heart Association (0865150F to A.J.E.), NIH (1DP02OD006460 to A.J.E.) and American Heart Association and ARCS predoctoral fellowships (to J.L.Y.).

Abbreviations

HA	Hyaluronic Acid
Pa	Pascal
PEGDA	poly(ethylene glycol) diacrylate
DG PBS	degassed phosphate buffered saline
AFM	atomic force microscopy
NMR	nuclear magnetic resonance
hpp	hours post polymerization
hpf	hours post fertilization
ELISA	enzyme-linked immunosorbent assay

References

1. Discher DE, Mooney DJ, Zandstra PW. Growth factors, matrices, and forces combine and control stem cells. Science 2009;324(5935):1673–1677. [PubMed: 19556500]
2. Saha K, Keung AJ, Irwin EF, Li Y, Little L, Schaffer DV, et al. Substrate modulus directs neural stem cell behavior. Biophys J 2008;95(9):4426–4438. [PubMed: 18658232]
3. Engler AJ, Sen S, Sweeney HL, Discher DE. Matrix elasticity directs stem cell lineage specification. Cell 2006;126(4):677–689. [PubMed: 16923388]
4. Huebsch N, Arany PR, Mao AS, Shvartsman D, Ali OA, Bencherif SA, et al. Harnessing traction-mediated manipulation of the cell/matrix interface to control stem-cell fate. Nat Mater 9(6):518–526. [PubMed: 20418863]
5. Lutolf MP, Hubbell JA. Synthetic biomaterials as instructive extracellular microenvironments for morphogenesis in tissue engineering. Nat Biotechnol 2005;23(1):47–55. [PubMed: 15637621]
6. Nelson CM, Bissell MJ. Of extracellular matrix, scaffolds, and signaling: tissue architecture regulates development, homeostasis, and cancer. Annu Rev Cell Dev Biol 2006;22:287–309. [PubMed: 16824016]
7. Deroanne CF, Lapiere CM, Nusgens BV. In vitro tubulogenesis of endothelial cells by relaxation of the coupling extracellular matrix-cytoskeleton. Cardiovasc Res 2001;49(3):647–658. [PubMed: 11166278]
8. Guo WH, Frey MT, Burnham NA, Wang YL. Substrate rigidity regulates the formation and maintenance of tissues. Biophys J 2006;90(6):2213–2220. [PubMed: 16387786]

NIH-PA Author Manuscript

NIH-PA Author Manuscript

NIH-PA Author Manuscript

9. Townes PL, Holtfreter J. Directed movements and selective adhesion of embryonic amphibian cells. J Exp Zool 1955;128(1):53–120.
10. Hay, ED. Cell biology of extracellular matrix. 2. New York: Plenum Press; 1991.
11. Montell DJ. Morphogenetic cell movements: diversity from modular mechanical properties. Science 2008;322(5907):1502–1505. [PubMed: 19056976]
12. Bird SD, Doevendans PA, van Rooijen MA, Brutel de la Riviere A, Hassink RJ, Passier R, et al. The human adult cardiomyocyte phenotype. Cardiovasc Res 2003;58:423–434. [PubMed: 12757876]
13. Sanger JW, Kang S, Siebrands CC, Freeman N, Du A, Wang J, et al. How to build a myofibril. J Muscle Res Cell Motil 2005;26(6–8):343–354. [PubMed: 16465476]
14. Shapira-Schweitzer K, Seliktar D. Matrix stiffness affects spontaneous contraction of cardiomyocytes cultured within a PEGylated fibrinogen biomaterial. Acta Biomater 2007;3:33–41. [PubMed: 17098488]
15. Jacot JG, McCulloch AD, Omens JH. Substrate stiffness affects the functional maturation of neonatal rat ventricular myocytes. Biophys J 2008;95(7):3479–3487. [PubMed: 18586852]
16. Engler AJ, Carag-Krieger C, Johnson CP, Raab M, Tang HY, Speicher DW, et al. Embryonic cardiomyocytes beat best on a matrix with heart-like elasticity: scar-like rigidity inhibits beating. J Cell Sci 2008;121(Pt 22):3794–3802. [PubMed: 18957515]
17. Berry MF, Engler AJ, Woo YJ, Pirolli TJ, Bish LT, Jayasankar V, et al. Mesenchymal stem cell injection after myocardial infarction improves myocardial compliance. Am J Physiol Heart Circ Physiol 2006;290(6):H2196–2203. [PubMed: 16473959]
18. Engler AJ, Griffin MA, Sen S, Bonnemann CG, Sweeney HL, Discher DE. Myotubes differentiate optimally on substrates with tissue-like stiffness: pathological implications for soft or stiff microenvironments. J Cell Biol 2004;166(6):877–887. [PubMed: 15364962]
19. Collinsworth AM, Zhang S, Kraus WE, Truskey GA. Apparent elastic modulus and hysteresis of skeletal muscle cells throughout differentiation. Am J Physiol Cell Physiol 2002;283(4):C1219–1227. [PubMed: 12225985]
20. Pasternak C, Wong S, Elson EL. Mechanical function of dystrophin in muscle cells. J Cell Bio 1995;128:355–361. [PubMed: 7844149]
21. Breitbach M, Bostani T, Roell W, Xia Y, Dewald O, Nygren JM, et al. Potential risks of bone marrow cell transplantation into infarcted hearts. Blood 2007;110(4):1362–1369. [PubMed: 17483296]
22. Krieg M, Arboleda-Estudillo Y, Puech PH, Kafer J, Graner F, Muller DJ, et al. Tensile forces govern germ-layer organization in zebrafish. Nat Cell Biol 2008;10(4):429–436. [PubMed: 18364700]
23. Hamburger V, Hamilton HL. A series of normal stages in the development of the chick embryo. J Morph 1951;88:49–62.
24. Hibbs RG. Electron microscopy of developing cardiac muscle in chick embryos. Am J Anat 1956;99(1):17–51. [PubMed: 13362124]
25. Zamir EA, Srinivasan V, Perucchio R, Taber LA. Mechanical asymmetry in the embryonic chick heart during looping. Ann Biomed Eng 2003;31(11):1327–1336. [PubMed: 14758923]
26. Shu XZ, Liu Y, Luo Y, Roberts MC, Prestwich GD. Disulfide cross-linked hyaluronan hydrogels. Biomacromolecules 2002;3(6):1304–1311. [PubMed: 12425669]
27. Tse JR, Engler AJ. Preparation of hydrogel substrates with tunable mechanical properties. Curr Protoc Cell Biol 2010;Chapter 10(Unit 10):16. [PubMed: 20521229]
28. Radmacher M. Studying the mechanics of cellular processes by atomic force microscopy. Methods Cell Biol 2007;83:347–372. [PubMed: 17613316]
29. Metters AT, Anseth KS, Bowman CN. A statistical kinetic model for the bulk degradation of PLA-b-PEG-b-PLA hydrogel networks: Incorporating network non-idealities. J Phys Chem B 2001;105(34):8069–8076.
30. Flory, PJ. Principles of polymer chemistry. Cornell University Press; 1953.
31. Humphrey JH. Antigenic properties of hyaluronic acid. Biochem J 1943;37(4):460–463. [PubMed: 16747669]

NIH-PA Author Manuscript

NIH-PA Author Manuscript

NIH-PA Author Manuscript

32. Burdick JA, Chung C, Jia X, Randolph MA, Langer R. Controlled degradation and mechanical behavior of photopolymerized hyaluronic acid networks. Biomacromolecules 2005;6(1):386–391. [PubMed: 15638543]

33. Serban MA, Yang G, Prestwich GD. Synthesis, characterization and chondroprotective properties of a hyaluronan thioethyl ether derivative. Biomaterials 2008;29(10):1388–1399. [PubMed: 18158182]

34. Serban MA, Scott A, Prestwich GD. Use of hyaluronan-derived hydrogels for three-dimensional cell culture and tumor xenografts. Curr Protoc Cell Biol 2008;Chapter 10(Unit 10):14. [PubMed: 18819087]

35. Dalby MJ, Gadegaard N, Tare R, Andar A, Riehle MO, Herzyk P, et al. The control of human mesenchymal cell differentiation using nanoscale symmetry and disorder. Nat Mater 2007;6(12): 997–1003. [PubMed: 17891143]

36. Metters AT, Bowman CN, Anseth KS. A statistical kinetic model for the bulk degradation of PLA-b-PEG-b-PLA hydrogel networks. J Phys Chem B 2000;104(30):7043–7049.

37. Engler AJ, Griffin MA, Sen S, Bonnemann CG, Sweeney HL, Discher DE. Myotubes differentiate optimally on substrates with tissue-like stiffness: pathological implications for soft or stiff microenvironments. J Cell Biol 2004;166(6):877–887. [PubMed: 15364962]

NIH-PA Author Manuscript
NIH-PA Author Manuscript
NIH-PA Author Manuscript

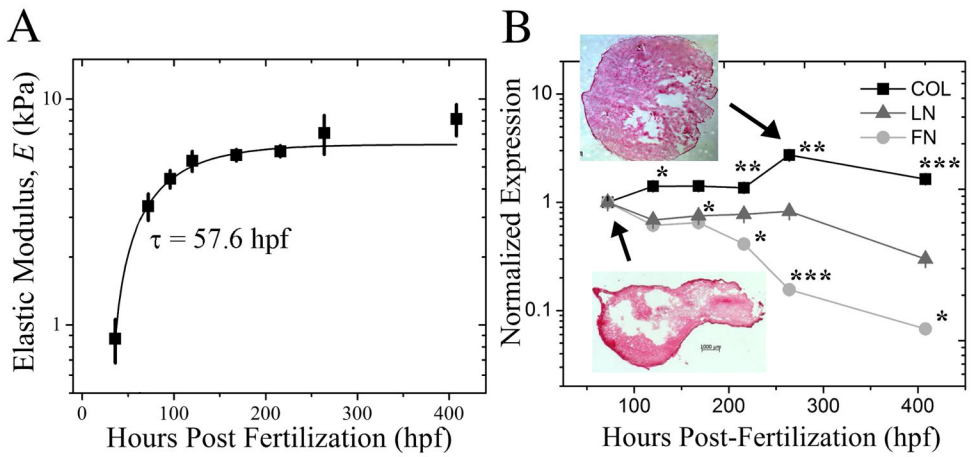

Fig. 1. Characterizing Myocardial Development in the Chicken Embryo

(A) Myocardial elastic modulus was measured by atomic force microscopy from 36 to 408 hpf. Data was fit with an exponential curve, which exhibited a time constant, τ, of 57.6 hpf as indicated. (B) qPCR quantification of myocardial collagen (black squares), laminin (grey triangles) and fibronectin (light grey circles) expression was normalized to the initial time point at 72 hpf and plotted as a function of developmental time. Inset images show tissue samples isolated at the indicated time points and stained with Picrosirius Red to indicate collagen localization (red). *$p < 0.05$, **$p < 0.01$, *** $p < 0.001$ compared to the initial time point.

NIH-PA Author Manuscript

NIH-PA Author Manuscript

NIH-PA Author Manuscript

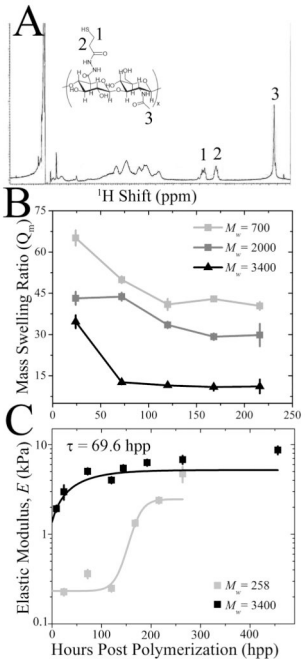

Fig. 2. HA Hydrogel Stiffening can be Tuned by Molecular Weight

(A) ^{1}H NMR spectroscopy of thiolated HA, indicating peaks from the thiolation (1, 2) and HA backbone (3) as shown on the inset schematic of thiolated HA. (B) Mass swelling ratio (Q_m) was examined over 216 hpp among HA hydrogels prepared from PEGDA of M_w ~ 700 Da (light grey), 2000 Da (dark grey) and 3400 Da (black). (C) Elastic modulus of HA hydrogels made of M_w ~ 258 and 3400 Da PEGDA was determined by AFM as a function of time. 3400 Da hydrogels were fit with an exponential curve exhibiting a time constants, τ, of 65 hpp. 258 Da hydrogels were hyperbolically fit to indicate slower crosslinking.

NIH-PA Author Manuscript

NIH-PA Author Manuscript

NIH-PA Author Manuscript

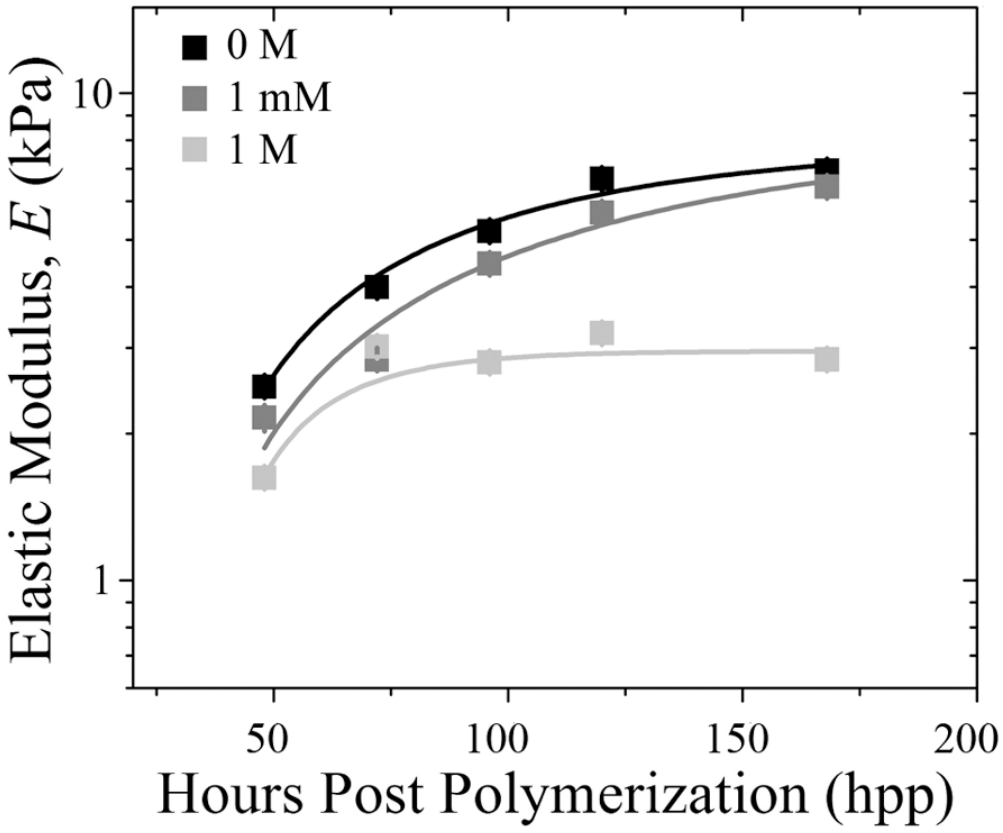

Fig. 3. Disulfide Bond Formation Does Not Substantially Contribute to Time-Dependent Stiffening

HA hydrogels made of M_w ~ 3400 Da PEGDA were polymerized, subsequently treated with 0 M (black), 1 mM (grey) and 1 M (light grey) DTT, and their elastic modulus was determined by AFM as a function of time. HA hydrogel data at 1 mM and 1 M were fitted with exponential curves, exhibiting time constants, τ, of 80 and 20 hpp, respectively.

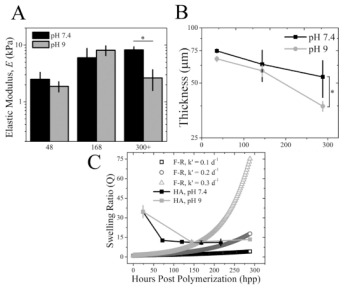

Fig. 4. HA Hydrogel Stiffening Initially Outcompetes Ester Hydrolysis

(A) HA hydrogel elastic modulus was measured in both pH conditions over time and was reduced only in pH 9 samples after 300+ hpp. *$p < 0.05$. (B) HA hydrogel thickness was examined over 288 hpp in pH 7.4 (black squares) and 9 (grey circles) by confocal microscopy. Modest hydrogel thinning was observed for pH 7.4 but was > 45% for pH 9. *$p < 0.005$. (C) Equilibrium mass swelling ratio of HA hydrogels at pH 7.4 (black) and 9 (light grey) was determined up to 288 hpp. Data is plotted as compared to a modified Flory-Rehner (F-R) model of hydrolysis for volumetric swelling where the F-R ester bond hydrolysis constant, k', was varied. $k' = 0.1\ \text{day}^{-1}$ (open black squares), $k' = 0.2\ \text{day}^{-1}$ (open dark grey circles) and $k' = 0.3\ \text{day}^{-1}$ (open light grey triangles).

NIH-PA Author Manuscript NIH-PA Author Manuscript NIH-PA Author Manuscript

NIH-PA Author Manuscript
NIH-PA Author Manuscript
NIH-PA Author Manuscript

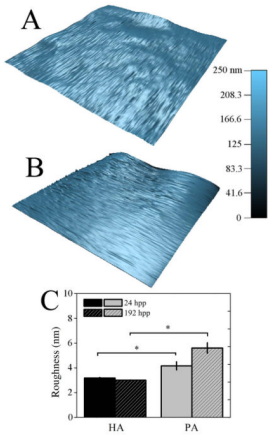

Fig. 5. HA Hydrogels Surface Topography Does Not Change Over Time

3-dimensional surface topography maps of HA (A) and PA (B) hydrogels at 196 hpp. (C) Surface roughness, as measured by root-mean-squared distance, was computed from topographical maps and plotted at both 24 and 192 hpp for HA and PA hydrogel systems. * $p < 0.05$.

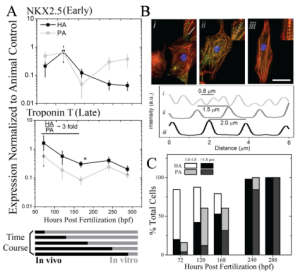

Fig. 6. Cardiomyocyte Maturation Is Improved on HA versus PA Hydrogels

(A) Cells from early through late myocardial development were plated onto HA (black squares) and PA (grey circles) hydrogels such that total cell age (*in vivo* and *in vitro*) was 312 hpf. Early and late cardiac markers NKX2.5 (top) and Troponin T (bottom) were measured by qPCR in cells plated on PA and HA hydrogels and normalized to the animal expression level at 312 hpf for the respective gene (see Supplemental Figure 5). Normalized expression below, at, or above 1 indicates lower, similar, or higher expression than the animal control, respectively. *$p < 0.05$ between HA and PA hydrogels. (B) Representative immunofluorescent images of cells stained for actin (red), alpha-actinin (green), and nuclei (blue) illustrate the stages of myofibril development in terms of striation length: premyofibrils at ~ 0.8 μm (i), maturing myofibrils at ~ 1.5 μm (ii), and mature myofibrils at ~2.0 μm (iii). Inset images indicate the myofibril that was examined in the corresponding intensity plot profile. Scale bar is 25 μm. (C) Cells were cultured in accordance to the time course in (A), and the percentage of cells containing nascent (1.0–1.8 μm; HA in white, PA in light grey) or mature myofibrils of (>1.8 μm; HA in black, PA in dark grey) was quantified. Premyofibrils (<1.0 μm), consist of the remaining percentage of cells, were not plotted. n > 25 cells were analyzed per time point per hydrogel.

NIH-PA Author Manuscript NIH-PA Author Manuscript NIH-PA Author Manuscript

NIH-PA Author Manuscript

NIH-PA Author Manuscript

NIH-PA Author Manuscript

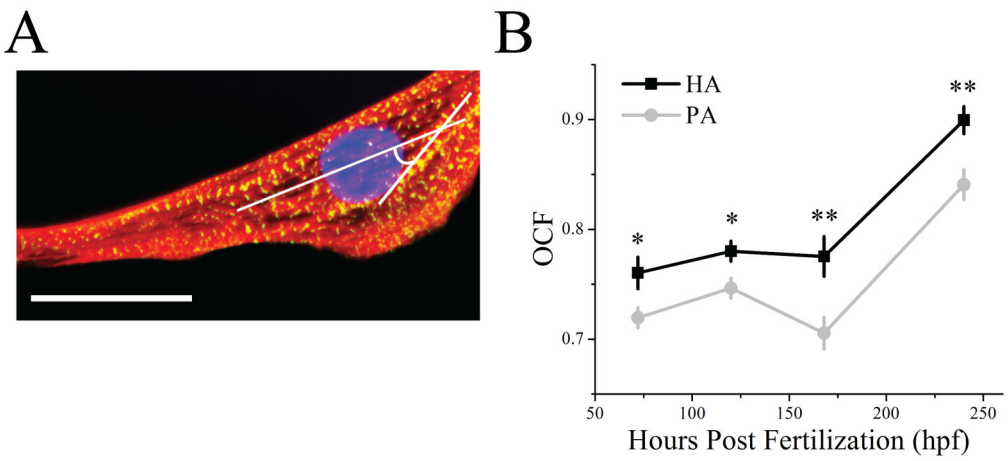

Fig. 7. Myofibrils are Most Oriented on HA Hydrogels

(A) Myofibril orientation was examined by calculating an orientation correlation function (OCF) where θ is the difference between the myofibril angle and the long axis of the cell as indicated in white in the image of a representative cell. Scale bar is 25 μm. (B) Quantification of OCF over time for cells cultured on HA (black squares) or PA hydrogels (grey circles). Note that OCF = 1 and 0.5 indicates parallel and diagonal alignment with respect to the long axis of the cell. * $p < 0.05$, ** $p < 0.005$ compared between HA and PA hydrogels.